

Native and Unfolded Cytochrome *c*—Comparison of Dynamics using 2D-IR Vibrational Echo Spectroscopy

Seongheun Kim,[†] Jean K. Chung,[†] Kyungwon Kwak,[†] Sarah E. J. Bowman,[‡] Kara L. Bren,[‡] Biman Bagchi,^{†,§} and M. D. Fayer^{*,†}

Department of Chemistry, Stanford University, Stanford, California 94305 and University of Rochester, Rochester, New York 14627-0216

Received: March 14, 2008; Revised Manuscript Received: May 16, 2008

Unfolded vs native CO-coordinated horse heart cytochrome *c* (h-cyt *c*) and a heme axial methionine mutant cyt *c*₅₅₂ from *Hydrogenobacter thermophilus* (*Ht*-M61A) are studied by IR absorption spectroscopy and ultrafast 2D-IR vibrational echo spectroscopy of the CO stretching mode. The unfolding is induced by guanidinium hydrochloride (GuHCl). The CO IR absorption spectra for both h-cyt *c* and *Ht*-M61A shift to the red as the GuHCl concentration is increased through the concentration region over which unfolding occurs. The spectra for the unfolded state are substantially broader than the spectra for the native proteins. A plot of the CO peak position vs GuHCl concentration produces a sigmoidal curve that overlays the concentration-dependent circular dichroism (CD) data of the CO-coordinated forms of both *Ht*-M61A and h-cyt *c* within experimental error. The coincidence of the CO peak shift curve with the CD curves demonstrates that the CO vibrational frequency is sensitive to the structural changes induced by the denaturant. 2D-IR vibrational echo experiments are performed on native *Ht*-M61A and on the protein in low- and high-concentration GuHCl solutions. The 2D-IR vibrational echo is sensitive to the global protein structural dynamics on time scales from subpicosecond to greater than 100 ps through the change in the shape of the 2D spectrum with time (spectral diffusion). At the high GuHCl concentration (5.1 M), at which *Ht*-M61A is essentially fully denatured as judged by CD, a very large reduction in dynamics is observed compared to the native protein within the ~100 ps time window of the experiment. The results suggest the denatured protein may be in a glassy-like state involving hydrophobic collapse around the heme.

I. Introduction

Protein folding is a fundamentally important problem that has been intensely investigated for decades.^{1–10} Although a great deal is known about protein folding, some of the most important issues remain unresolved. The theoretical models of protein folding can be broadly divided into two categories. The first model is that protein folding proceeds through a unique predetermined sequence of metastable intermediate states of increasingly lower energy until the native state is reached.^{2–5} The native state is assumed to be the state of lowest free energy. The alternative folding funnel model^{7,8,11,12} based on energy landscape considerations advocates a multitude of pathways and no unique sequence of intermediate states. The driving force in the funnel model is also the free energy bias toward the native state, but entropy considerations are included in the description of stabilization. While experimental results have been proposed in favor of both the models,^{6,10} it is fair to say that it is not clear which model is correct or whether either model is uniquely correct. Indeed, treatments of protein folding data benefit from consideration of both of these models which are not mutually exclusive.

A major difficulty in experimentally addressing the protein folding problem is the proper identification and characterization

of non-native conformational states on the folding energy landscape. These conformations can be short lived, which can inhibit thorough examination. To improve characterization of folding intermediates, considerable research has been directed toward unfolding of proteins from their native states. The utility of this approach is that a non-native state can be stabilized by use of an appropriate amount of a denaturant such as guanidinium hydrochloride (GuHCl) or urea. These denaturants are known to destabilize proteins in different ways.^{13–17} The guanidinium cation may disrupt salt bridges and other Coulombic interactions within the protein.^{18,19} In contrast, urea is uncharged and generally denatures a protein by disrupting its secondary structures and operates at higher concentrations than GuHCl. By using a particular denaturant it is possible to create an ensemble of non-native states of nearly identical characteristics which can then be probed experimentally.

Because of their relative simplicity and high solubility, proteins in the cytochrome *c* (cyt *c*) family have served as important model systems in protein folding studies using a host of optical and magnetic resonance techniques.^{13,17,20–33} Class I cyts *c* proteins are soluble and monomeric with a single heme group covalently bound to a Cys-X-X-Cys-His motif in which the two Cys form thioether linkages to the heme and the His binds the heme iron.³⁴ Figure 1 displays the active site with the Cys linkages shown. A range of experiments on cyts *c* have been directed toward distinguishing between the sequential model and the folding funnel model and characterizing the non-native states. A series of papers by Englander and co-workers (who used a hydrogen exchange method) has indicated the

* To whom correspondence should be addressed. E-mail: fayer@stanford.edu.

[†] Stanford University.

[‡] University of Rochester.

[§] Permanent address: Solid State and Structural Chemistry Unit, Indian Institute of Science, Bangalore 560 012, India.

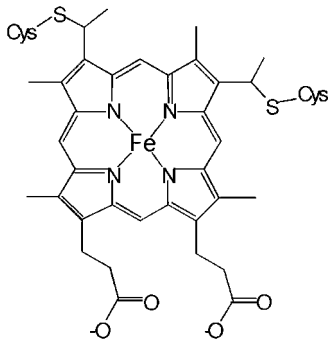


Figure 1. Active site of Class I cyt *c* with a single heme group covalently bound to a Cys-X-X-Cys-His motif in which the two Cys form thioether linkages to the heme.

existence of a definite pathway of unfolding through a well-defined sequence of intermediate states.^{10,35} These studies seem to run counter to the folding funnel picture. Subsequent theoretical studies by Wolynes and co-workers suggested that the hydrogen exchange experiments can be explained within the folding funnel picture.⁶ Comparative studies of the folding of Class I cyts *c* from different subfamilies suggest that proteins in this class share a common folding nucleus, which translates to a common folding mechanism.^{26,36}

Class I cyts *c* as a group are among the most actively studied proteins in the context of chemical and thermal denaturation, in which the heme plays an important role and serves as a valuable probe.^{13,16,17,21–30,37–41} The thioether bonds ensure that the heme prosthetic group is closely associated with the protein in the native and unfolded configurations. The heme is axially ligated by side chains of a histidine and a methionine. The methionine–iron bond may be disrupted by binding of exogenous ligands which serve as probes of the physical properties of the heme and its environment.⁴² Alternatively, mutation of the axial methionine to nonligating alanine creates a site for ligand probes to bind the heme iron.⁴³

In this paper we report a new approach to studying the denaturation of two different Class I cyts *c*. The stretching mode of CO bound to the reduced Fe of these cyts *c* is studied as a function of GuHCl concentration using infrared absorption spectroscopy and ultrafast two-dimensional infrared (2D-IR) vibrational echo spectroscopy. Experiments are conducted on CO-coordinated ferrous cyt *c*₅₅₂ mutant from *Hydrogenobacter thermophilus* (in which the heme axial ligand Met61 is replaced with Ala, *Ht*-M61A) and on the CO derivative of ferrous horse heart cyt *c* (h-cyt *c*). Both are Class I cyts *c* proteins, but h-cyt *c* is from the mitochondrial cyt *c* subfamily, and *Ht* cyt *c*₅₅₂ is from the cyt *c*₈ subfamily (sometimes called the cyts *c*₅₅₁).⁴⁴ The folding of these proteins has been proposed to involve a common folding nucleus and mechanism resulting from their similar folding topology.^{26,36}

The linear absorption spectra display a single CO band for the native proteins that shifts to lower frequency as the GuHCl concentration is increased. For h-cyt *c*, a comparison of the CO absorption peak shift with GuHCl concentration is almost identical to the concentration dependence of the CD data, demonstrating that the CO vibration is sensitive to the structural changes induced by the denaturant. In addition to the absorption band shift with increasing concentration, the CO band develops a shoulder and then becomes a much broader band at high (>5 M) GuHCl concentration. The CO band is inhomogeneously broadened, and the width reflects the range of structural configurations available to the protein. The increase in width

when the protein is unfolded indicates the existence of a broader range of structures in the denatured state than in the native state.

The 2D-IR vibrational echo experiments are conducted on the CO bound to the *Ht*-M61A ferrous heme. 2D-IR vibrational echo spectroscopy^{45–47} can probe protein conformational fluctuations under thermal equilibrium conditions on timescales ranging from subpicosecond to ~100 ps or longer.^{48–53} 2D-IR vibrational echo spectroscopy reports on protein dynamics that occur on fast timescales. The method has recently been applied to biological problems^{54,55} including the study of model enzymes,^{56,57} protein unfolding,⁵⁰ peptide dynamics in membranes,⁵¹ and protein equilibrium fluctuations in aqueous and confined environments.^{48,49,52,53,58}

Here we employ 2D-IR vibrational echo spectroscopy to examine the equilibrium structural fluctuations of different states of *Ht*-M61A by observing the change in the 2D lineshapes with time for three samples: the native protein and the protein in low- and high-concentration GuHCl. Within the time window of the experiments (subpicosecond to ~100 ps), the native protein displays considerable fast structural dynamics with approximately >50% of the accessible structures being sampled in <100 ps. However, the unfolded protein formed at high GuHCl concentration (5.1 M) shows a dramatic change in the structural dynamics with only ~15% of the protein configurations being sampled in <100 ps. There is a significant decrease in the homogeneous (motionally narrowed) contribution to the 2D spectra and a substantial decrease in the fraction of structures sampled on the longer time scale (100 ps). The changes indicate that the unfolded state may be in a compact, hydrophobicity driven collapsed glassy state.

II. Experimental Procedures

A. Sample Preparation. Preparation of *Ht*-M61A utilized an *E. coli*-based expression system.^{59,60} Molecular biology procedures and materials and preparation of *Ht*-M61A are described in detail elsewhere.^{20,61,62} To prepare aqueous samples of CO-ligated *Ht*-M61A for IR studies, 10 mg of lyophilized protein was dissolved in 1.0 mL of pD 7.4 phosphate buffer (50 mM) in D₂O. The solutions were reduced with a 5-fold excess of dithionite (Aldrich) and stirred under a CO atmosphere for 1 hour. The solutions were centrifuged at 3000 relative centrifugal force for 15 min through a 0.45- μ m acetate filter (Pall Nanosep MF) to remove particulates. CO-ligated *Ht*-M61A was then denatured by adding GuHCl phosphate buffer to obtain final concentrations of 3.2 and 5.1 M GuHCl. The samples were further concentrated by repeated centrifugation (Eppendorf 5415D) over modified polyethersulfone membranes (Pall Nanosep 3K Omega) to a final protein concentration of 6–8 mM. The sample was then placed in a sample cell with CaF₂ windows and a 56 μ m Teflon spacer.

Horse heart cyt *c* (Type VI from Sigma) in 6 M GuHCl was prepared by dissolving 6 mM protein in deoxygenated GuHCl and 50 mM potassium phosphate (pD 7.4). The protein was reduced and ligated with CO as described above. Samples in the range of 0.0003–5.8 M GuHCl were prepared by combining the h-cyt *c*/6 M GuHCl solution with a 50 mM phosphate buffer solution. To remove light scattering sources such as dust particles, samples were filtered through a 0.45- μ m acetate filter (Pall Nanosep MF) and then concentrated by centrifugation to a final protein concentration of 6–8 mM before loading in a gastight 50 μ m path length sample cell with CaF₂ windows.

B. 2D-IR Vibrational Echo Spectroscopy. The experimental setup is similar to those described previously.^{46,47,63} Briefly, the mid-IR pulses with center frequency adjusted to

the absorption frequency of each protein sample were generated by an optical parametric amplifier pumped with a regeneratively amplified Ti:Sapphire laser. The bandwidth and duration of the mid-IR pulses were 150 cm^{-1} and 110 fs, respectively. Three mid-IR pulses were sequentially time delayed before they were crossed and focused in the sample. The vibrational echo pulse generated in the phase-matched direction was made collinear with a local oscillator pulse, dispersed through a monochromator, and detected with a 32-element HgCdTe array detector. The signal was interfered with the local oscillator to obtain full time, frequency, and phase information from the vibrational echo wave packet.

The 2D-IR spectrum is obtained as a function of three variables: the emitted vibrational echo frequencies, ω_m , and the variable time delays between the first and second pulses (τ) and the second and third pulses (T_w , "waiting" time). The 2D spectrum at each T_w was obtained by numerically Fourier transforming the τ scan data at each emission frequency, ω_m , to give the ω_τ axis. The 2D-IR data presented below are plotted as a function of ω_τ and ω_m .

C. Circular Dichroism Spectroscopy. Samples of CO-ligated *Ht-M61A* for circular dichroism (CD) spectroscopy were prepared as described above, except that $10\ \mu\text{M}$ protein samples were prepared in 50 mM sodium phosphate buffer in H_2O . GuHCl solutions were prepared from a stock solution of 8.2 M GuHCl in 50 mM sodium phosphate buffer, pH 7.0, with a final range of GuHCl concentrations from 0.0 to 7.0 M. Refractive index measurement was used to determine the GuHCl concentration of each sample as described.⁶⁴ The pH of each sample was adjusted to 7.0 prior to data collection. CD measurements were performed on an Aviv Instruments model 202 spectropolarimeter using a quartz cell with 0.100 cm path length. CD spectra of samples were recorded every 0.5 nm over a range of 224–220 nm with an averaging time of 5 s and a bandwidth of 1.00 nm. The change in the CD signal at 222 nm was analyzed to follow the unfolding of the protein at different GuHCl concentrations. The concentration used for the CD experiments is very low compared to those used for the vibrational echo experiments. A protein concentration study of the denaturation of h-cyt *c* with GuHCl measured with CD over the protein concentration range 0.014–0.224 mM showed no dependence on concentration.²⁹ The highest concentration used in that study is well below the concentration employed in the vibrational echo experiments, but it suggests that the CD results will be unchanged at even higher concentrations. NMR experiments carried out on high concentrations (1–3 mM) of the wild-type *Ht-cyt c* show no evidence of aggregation.⁶⁵ Furthermore, as discussed below, the denaturation studies using IR absorption experiments on h-cyt *c* and *Ht-M61A* as a function of GuHCl concentration show the same denaturation curves as found with CD. These IR absorption studies were performed on samples with the same high concentration used in the vibrational echo experiments. Therefore, the high protein concentrations used in the IR experiments do not appear to influence the results.

III. Results

A. Time-Independent Spectroscopy. A complete set of CO-ligated h-cyt *c* IR absorption spectra of the CO stretching mode were taken as a function of GuHCl concentration, and a small number of spectra were taken on *Ht-M61A*. Most of the absorption experiments were conducted on h-cyt *c* because it was readily available.

The heme iron of h-cyt *c* is axially ligated with His18 and Met80 to yield a six-coordinated form under physiological

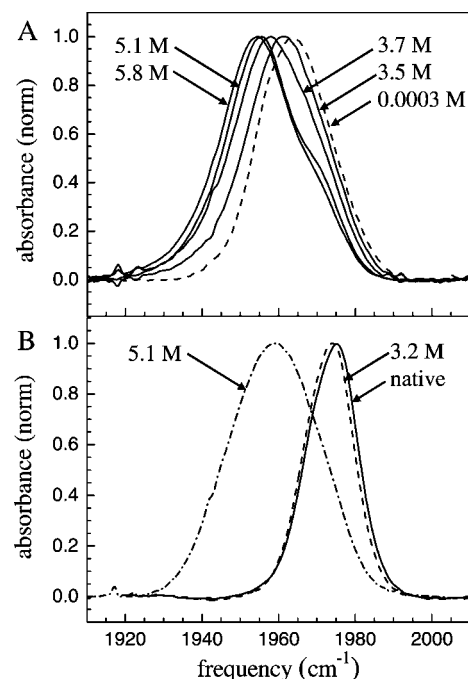


Figure 2. Vibrational absorption spectra of the stretching mode of CO bound to horse heart cyt *c* (A) and the mutant *Ht-M61A* (B) at room temperature, pH 7.4, for various concentrations of GuHCl.

conditions. When the protein is denatured under high GuHCl or urea concentration, Met80 dissociates from the heme and heme iron (Fe^{2+}) can bind small ligands such as CO and NO tightly in the denatured state.²⁹ When the denaturant is diluted, the denatured protein with CO bound refolds to form CO-ligated ferrocyt *c*.²⁹ Studies have shown that unfolded h-cyt *c* at neutral pH displays non-native ligation to the heme by His26 and His33.^{13,29,66–68} Partly as a result of formation of this improperly ligated structure, the refolding of h-cyt *c* at neutral pH is quite complex. However, binding CO to heme in the unfolded state eliminates the possibility of forming improperly ligated structures.

Figure 2A displays several spectra of the CO stretch of h-cyt *c*-CO. As the concentration of GuHCl increases, the band shifts to the red (lower frequency) and broadens. In addition, there is a shoulder on the blue side of the line for the higher concentrations that decreases as the concentration increases further. Figure 2B shows spectra of the mutant protein M61A-CO for the three GuHCl concentrations that were studied with the 2D-IR vibrational echo experiments discussed below.

An earlier study using a native *Ht-M61A* FT-IR spectroscopy at room temperature reported a single CO stretching band at 1974 cm^{-1} with 14.7 cm^{-1} fwhm.²⁰ In that study, the double mutant *Ht-M61A/Q64N* was prepared to replace Gln64 with Asn in addition to the M61A mutation. According to an NMR study,²⁰ Gln64 in *Ht-M61A* is expected to be oriented out of the heme pocket to be consistent with a non-hydrogen-bonding interaction with the CO ligand, while Asn64 is oriented into the active site in *Ht-M61A/Q64N* to donate a hydrogen bond. The CO band in a native *Ht-M61A* is attributed to a conformation in which the distal Gln64 is positioned out of heme pocket. Thus, the CO band position in *Ht-M61A* is higher in frequency ($\sim 9\text{ cm}^{-1}$) than that in *Ht-M61A/Q64N*.

With *Ht-M61A*, again there is a red shift and broadening as the concentration of GuHCl increases. While the trend in peak positions and widths is similar, they are not identical. For h-cyt *c* the spectrum shifts from 1963 cm^{-1} (0.0003 M) to 1955 cm^{-1} (5.8 M), while for *Ht-M61A* the spectrum shifts from 1975 cm^{-1} (native)

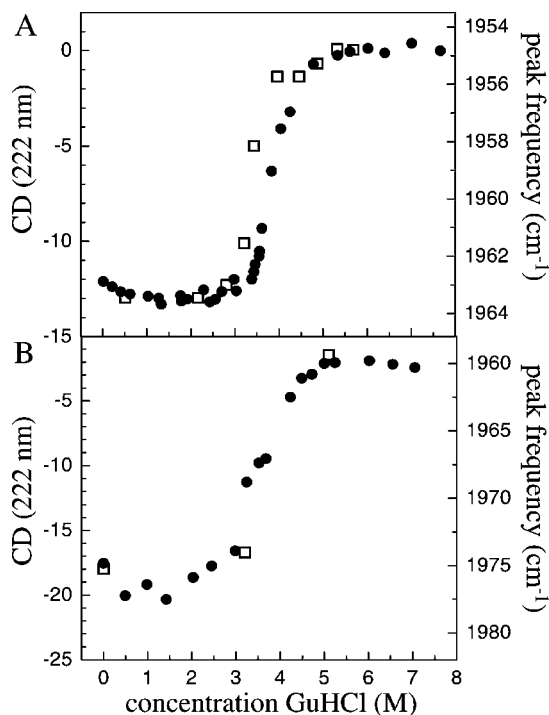


Figure 3. CD data (filled circles) and CO stretching mode absorption band shift for CO bound to (A) horse heart cyt *c* and (B) the mutant *Ht-M61A* as a function of GuHCl concentration. The CD data for horse heart cyt *c* is from ref 29. The close correspondence between the CD data and the vibrational band shift data shows that the CO vibrational frequency is sensitive to the same global structural changes as CD.

to 1959 cm^{-1} (5.1 M). In addition, the highest concentration h-cyt *c* peak has a width of 25 cm^{-1} fwhm, while for *Ht-M61A* it is 28 cm^{-1} fwhm. Using CO as a reporter, *Ht-M61A* has a somewhat greater response to unfolding than does h-cyt *c*. The CO peak for *Ht-M61A* shifts further to the red at high GuHCl concentration and the high-concentration absorption bandwidth is larger.

Figure 3A displays two types of data as a function of GuHCl concentration for h-cyt *c*. The squares are the peak positions of the CO absorption band. The circles are CD data from the literature.²⁹ Two data sets have been scaled so that the amplitudes match at the highest and lowest GuHCl concentration. The change in the peak position with GuHCl concentration closely mimics the CD data, suggesting that the CO vibrational band frequency is sensitive to global unfolding. Figure 3B shows CD data taken on *Ht-M61A* (circles). The signal-to-noise ratio for the CD of *Ht-M61A* is not as good as for the spectra of h-cyt *c*. The squares are the *Ht-M61A*-CO peak positions for the three concentrations studied below with 2D-IR experiments. While there are only three points, they appear to be consistent with the CD data. In the future this plot will be filled in. For now, we will assume that the vibrational frequency of *Ht-M61A* is sensitive to the extent of denaturation in the same manner as h-cyt *c* and the global changes in the protein structure monitored by CD. It is important to note, however, that protein unfolding is complex; *Ht* cyt *c* unfolding involves a well-populated intermediate non-native state,²⁶ and although h-cyt *c* unfolding can be approximated with a two-state model, close examination has shown it to be highly heterogeneous.^{16,32,69,70} Thus, the interpretation of how denaturation impacts the CO stretch will be revisited as models of folding and our understanding of 2D-IR as a probe of folding evolve.

B. 2D-IR Vibrational Echo Spectroscopy. 2D-IR vibrational echo spectroscopy directly examines structural degrees

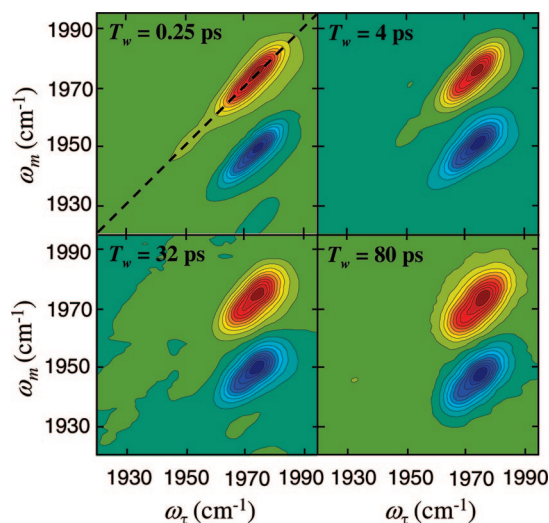


Figure 4. 2D-IR vibrational echo spectra of the stretching mode of CO bound to *Ht-M61A* at several delays, T_w . The diagonal is the dashed line shown in the upper left panel. The bands on the diagonal are positive going, and the off-diagonal bands are negative going. As T_w increases, the shape of the 2D spectrum changes, becoming less elongated. The change in shape with T_w is caused by protein structural evolution-induced spectral diffusion.

of freedom on very fast time scales, ~ 100 fs to ~ 100 ps. The vibrational echo signals are recorded by scanning τ at fixed T_w to produce a 2D spectrum. T_w is then increased, and another spectrum is taken. As T_w increases, the peak shapes in the 2D-IR spectra change. These changes are directly related to the structural evolution of the protein through the influence of the changes in structure on the CO stretch frequency. Very qualitatively, the 2D-IR experiment can be viewed as follows. The first and second pulses act to label the initial frequencies of the molecular oscillators. Between the second and third pulses, structural evolution causes the initially labeled frequencies to change (spectral diffusion). The third pulse ends the evolution period, and the vibrational echo signal reads out the final frequencies of the initially frequency-labeled molecular oscillators. As T_w increases, there is more time for structural evolution to occur and, therefore, larger frequency changes. The structural evolution (frequency change) is reflected in the changes of peak shape of the 2D-IR spectra. The 2D-IR vibrational echo experiments have been reviewed recently.^{45–47}

Figure 4 displays 2D-IR vibrational echo spectra for native *Ht-M61A* at several times, T_w . In the $T_w = 0.25$ ps panel, the dashed line is the diagonal. There are two bands in each of the spectra. The band on the diagonal (positive going) arises from the 0–1 vibrational transition of the CO stretching mode. The band below it, off-diagonal (negative going), arises from vibrational echo emission at the 1–2 transition frequency, which is shifted to lower frequency by the anharmonicity of the vibrational potential.^{71,72} Both types of bands provide the same information. Therefore, we will focus on the 0–1 transition band on the diagonal.

At short T_w , the peaks in the 2D-IR spectra reveal a strong elongation along the diagonal. For the shortest two T_w s shown, there is a long tail going to low frequency. This tail arises from a low-amplitude band in the absorption spectrum that is centered at ~ 1953 cm^{-1} . This peak has a shorter lifetime than the main band further to the blue. It has decayed and is not visible in the $T_w = 32$ ps spectrum. The important feature for the main band is that as T_w increases the shape becomes less elongated along the diagonal. Elongation along the diagonal is caused by

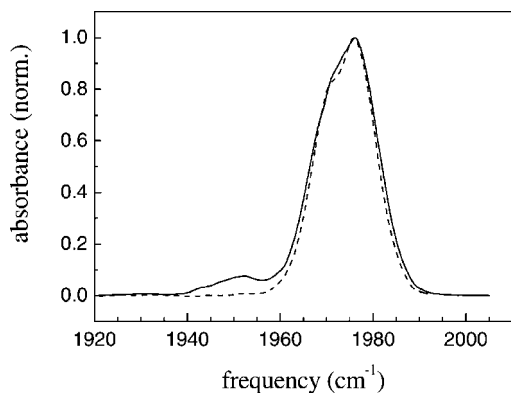


Figure 5. Native *Ht*-M61A-CO spectra produced by cutting the 2D vibrational echo spectrum along the diagonal at two T_w s: (solid curve) $T_w = 0.5$ ps; (dashed curve) $T_w = 32$ ps. The data show that the native protein has three conformational substates (see text).

inhomogeneous broadening. At short time there are many structural configurations of the protein that have not yet been sampled by structural evolution. As time increases, structural evolution causes spectral diffusion, resulting in the change in shape. The longest time for the measurements is limited to a few T_1 's, where T_1 is the vibrational lifetime. Here data could be collected out to 120 ps. The spectrum is sensitive to structural fluctuations that are a few times the longest T_w measured because some portion of slower fluctuations will occur in the experimental window if their time scale is not too slow.⁷³ If there were no time limit on the measurement, then the 2D bands would eventually become round when spectral diffusion is complete, that is, when all possible structural configurations have been sampled.

Figure 5 displays spectra that are slices along the diagonal of the 2D spectra taken at two times: $T_w = 0.25$ (solid curve) and 32 ps (dashed curve). The two spectra have been normalized. At short time (0.25 ps), the small peak at ~ 1953 cm^{-1} is apparent. At long time (32 ps), the 1953 cm^{-1} peak is absent because it has a shorter lifetime. For CO bound to hemes or metalloporphyrins it is well documented that the CO vibrational lifetime decreases essentially linearly as the frequency of the transition decreases.^{74–76} In both Figures 2B and 5, the main band for the native protein shows some asymmetry. In Figure 5 the 2D diagonal cut at 32 ps strongly suggests that there are two substates responsible for the absorption band. The difference between the 2D diagonal spectrum at 0.25 and 32 ps arises from a slight difference in the lifetimes of the two substates. The spectra shown in Figure 5 indicate that the native *Ht*-M61A protein exists in three conformational substates.

The change of peak shapes in the 2D-IR spectra with increasing T_w (see Figure 4) can be employed to determine the time scales and amplitudes of various contributions to the structural evolution of the protein using methods based on diagrammatic perturbation theory.^{77,78} The frequency–frequency correlation function (FFCF) connects the experimental observables to the underlying dynamics. The FFCF is the joint probability distribution that the frequency has a certain initial value at $t = 0$ and another value at a later time t . As the structure evolves, the initial frequencies of the protein bound COs change and the FFCF decays. Once the FFCF is known, all linear and nonlinear optical experimental observables can be calculated by time-dependent diagrammatic perturbation theory.^{77,78} Conversely, the FFCF can be extracted from 2D-IR spectra with additional input from linear FT-IR absorption spectra. In general, to determine the FFCF from 2D-IR and linear FT-IR spectra,

full calculations of linear and nonlinear third-order response functions are performed iteratively until the calculation results converge to the experimental results.⁷⁹

Here, the center line slope (CLS) method is employed.^{80,81} The CLS method is an approach for extracting the FFCF from the T_w dependence of the 2D-IR spectra that is accurate and much simpler to implement numerically than iterative fitting methods with calculations of all response functions based on time-dependent diagrammatic perturbation theory. Furthermore, the CLS provides a more useful quantity to plot for visualizing differences in the dynamics as a function of GuHCl concentration than a series of full 2D-IR spectra.^{52,53,80,81} In the CLS method employed here, frequency slices through the 2D-IR spectrum parallel to the ω_m axis at various ω_τ s are projected onto the ω_m axis.^{80,81} These projections are a set of spectra with peak positions, ω_m^{max} , on the ω_m axis. The plot of ω_m^{max} vs ω_τ forms a line called the center line. In the absence of a homogeneous contribution to the 2D-IR spectrum (see below), the peak shape in the 2D-IR spectrum at $T_w = 0$ ps would be essentially a line along the diagonal at 45° . The slope of this center line would be 1. At very long time, the peak shape in the 2D-IR spectrum becomes symmetrical and the center line is horizontal (slope is zero). It has been shown theoretically that the normalized FFCF is equal to the T_w dependence of the slope of the center line (CLS).^{80,81} Therefore, the CLS will vary from a maximum value of 1 at $T_w = 0$ ps to a minimum value of 0 at a sufficiently long time. It has also been shown theoretically that by combining the analysis of the CLS with the linear FT-IR absorption spectrum, the full FFCF can be obtained, including the T_w -independent homogeneous component.^{80,81}

A homogeneous contribution to the peak shape in the 2D-IR spectra and the line shape of the linear FT-IR absorption spectra can arise from three sources: very fast structural fluctuations that produce a motionally narrowed contribution to the FFCF,^{79,82} vibrational population relaxation, and orientational relaxation. Because the rotational diffusion time of the protein is long relative to the vibrational lifetime, the contribution from orientational relaxation is negligible. The vibrational population relaxation times (vibrational lifetimes) were measured independently using IR pump–probe experiments. The lifetime contribution to the homogeneous line width is small. Motional narrowing occurs when there is some portion of the structural fluctuations that are extremely fast, such that $\Delta\tau < 1$, where τ is the time scale of the fast fluctuations and Δ is the amplitude of the associated frequency fluctuations. Motionally narrowed fluctuations produce a Lorentzian contribution to both the 2D-IR spectrum and the linear FT-IR absorption spectrum. The T_w -independent homogeneous contribution manifests itself by broadening the 2D-IR spectrum along the ω_τ axis even at $T_w = 0$ ps. This homogeneous broadening reduces the initial value of the CLS to a number less than 1, which permits its determination.

A multiexponential form of the FFCF, $C(t)$, is used to model the multitime scale dynamics of the structural evolution of the protein systems. This form has been used previously for the analysis of a number of heme proteins.^{20,46,48,49,52,53,58,62,83} The FFCF has the form

$$C(t) = \sum_{i=1}^n \Delta_i^2 e^{-t/\tau_i} + \Delta_s^2 \quad (1)$$

The Δ_i and τ_i terms are the amplitudes and correlation times, respectively, of the frequency fluctuations induced by protein structural dynamics. τ_i reflects the time scale of a set of structural fluctuations, and the Δ_i is the range of CO frequencies sampled due to those structural fluctuations. The experimental time

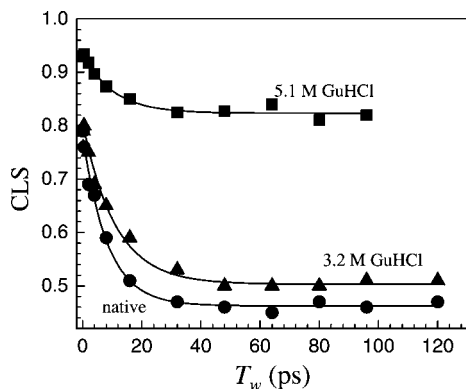


Figure 6. Center line slope (CLS) data for native *Ht*-M61A-CO in aqueous solution and in 3.2 and 5.1 M GuHCl solutions. The dynamics in the ~ 100 ps experimental time window of the denatured protein (5.1 M GuHCl) are substantially changed from those of the native protein.

window is a few T_1 's because lifetime decay reduces the signal to zero. The 2D-IR vibrational echo experiment is sensitive to fluctuations a few times longer than this window⁷³ because some portion of slower fluctuations will occur in the experimental window if their time scale is not too slow. Protein structural dynamics that are sufficiently slow will appear as static inhomogeneous broadening, which is reflected in $C(t)$ by Δ_s , a static term. In obtaining the FFCF from the data, Δ_i and τ_i are determined. However, for a motionally narrow term ($\Delta\tau < 1$), only the product, $\Delta^2\tau = 1/T_2^*$, can be obtained. T_2^* is called the pure dephasing time. The pure dephasing time is obtained using $1/T_2 = 1/T_2^* + 1/2T_1$, where T_2 is determined from the CLS with the linear absorption spectrum^{80,81} and T_1 is obtained from IR pump-probe experiments. The pure dephasing line width is $\Gamma = 1/\pi T_2^*$.

Figure 6 displays CLS data for native *Ht*-M61A and for the protein in 3.2 and 5.1 M GuHCl solutions. As can be seen in Figure 3, 3.2 M is at the onset of the denaturation while at 5.1 M denaturation is essentially complete. As will be discussed below, the FFCF for all three samples is well described by three terms in eq 1. As discussed above, the difference between 1 and the $T_w = 0$ value of the CLS is related to the homogeneous component of the dynamics. All three curves show a deviation from 1 at $T_w = 0$. At relatively short times, < 40 ps, there is a decay. Following the decay, the CLS becomes horizontal. The horizontal portion of the data is described by the static term in the FFCF and indicates that there are dynamics that are too slow to be observed within the time frame of the experiment.

First consider the CLS data for the native state qualitatively. During the 120 ps of observation, the CLS has decayed to 0.46. This means that over one-half of the spectroscopic line has been sampled by spectral diffusion. Part of this sampling is described by the homogeneous component. The homogeneous component is caused by exceedingly fast fluctuations on an atomic distance scale that may be thought of as thermally populated low-frequency vibrations.^{58,62,83} The dynamics on the tens of picosecond time scale involve much larger distance scales. A reasonable question is: what is the distance scale of motions that occur on these time scales? Incoherent quasielastic neutron scattering experiments on native bovine α -lactalbumin observed collective motions on the tens of picosecond time scale.⁸⁴ The correlation length for such fluctuations was reported to be 18 Å.⁸⁴ Therefore, the fluctuations that cause the decay of the CLS should represent motions of amino acids and collections of amino acids. The fact that the CLS becomes flat and that 46% of the inhomogeneous absorption line is not sampled within

TABLE 1: FFCF Parameters and Vibrational Lifetimes, T_1 , of the CO Band Bound to *Ht*-M61A^a

GuHCl conc.	Γ (cm ⁻¹)	τ_1 (ps)	Δ_i (cm ⁻¹)	Δ_s (cm ⁻¹)	T_1 (ps)
0.0 M	2.7 (22%)	8	4.2 (32%)	3.9 (46%)	29
3.2 M	2.5 (21%)	11	4.0 (29%)	3.5 (50%)	27
5.1 M	1.5 (7%)	10	4.7 (11%)	10.3 (82%)	23

^a Percentages are fractional contributions to the absorption line-widths.

the experimental time window means that approximately one-half of the accessible protein structural configurations interconvert on times scales significantly slower than 100 ps.

At the onset of denaturation (see Figure 6, 3.2 M GuHCl), the CLS changes but not by a great deal. The absorption spectrum (Figure 2B) is also almost the same as that of the native protein. Quantitative analysis of the data (see below) clearly delineates the small differences. However, the fully denatured protein (see Figure 6, 5.1 M GuHCl) shows dramatic changes from the native protein. The absorption spectrum is significantly different (see Figure 2B). In the CLS data, the homogeneous component is substantially reduced and the decay plateaus with $< 20\%$ of the spectroscopic line sampled. Therefore, on time scales of 100 ps there is a substantial change, the nature of which is discussed below.

The CLS decay results are quantified in Table 1. The table gives the parameters obtained from the CLS determination of the FFCF and the vibrational lifetime, T_1 , for each sample. The numbers in parentheses give the fraction of the particular contribution of the FFCF to the entire absorption line width. There are three terms in the FFCF (see eq 1). The first data column has the values of the pure dephasing linewidths, $\Gamma = 1/\pi T_2^*$. This component of the FFCF is determined by the difference between 1 and the $T_w = 0$ value in Figure 6. The next two columns are the decay constant and the amplitude factor that give rise to the decays that are seen in all three curves in Figure 6. The column labeled Δ_s is the amplitude of the static term, which sets the value of the long time plateau in the data. Comparing the results for the native protein (0.0 M GuHCl) to the protein at the onset of denaturation (3.2 M GuHCl), as can be seen from the CD and IR spectral shift data in Figure 3, the FFCF parameters are very similar except for τ_1 . The decay time τ_1 is longer for the slightly denatured protein, and Δ_s is a little larger. These differences can be seen in the data in Figure 6.

As can be seen in Figure 6, the large change in the dynamics occurs when the protein is fully denatured in 5.1 M GuHCl. Looking at the parameters in Table 1, the pure dephasing line width, Γ , becomes much narrower (T_2^* becomes longer) by almost a factor of 2. The decay time constant, τ_1 , is slower than in the native protein, although it does not change significantly from the value in 3.2 M GuHCl. In addition to the large change in the homogeneous component, the other large change is in the amplitude of the static term, Δ_s . This term goes from < 4 cm⁻¹ to > 10 cm⁻¹. For the denatured protein, the static term is responsible for 82% of the absorption line width compared to 46% for the native protein. This is seen in Figure 6 as the much higher value for the plateau for the denatured protein. The results demonstrate that denaturation changes the dynamics within the experimental window. The increase in the inhomogeneous line width shows that there are a wider range of structures in the denatured state, and within the time window of the experiment, a smaller fraction of these structures are sampled compared to the native state. Denaturation causes a large fraction of the dynamics to occur on time scales that are long compared to several hundred picoseconds because measurements within the

time window of ~ 100 ps are sensitive to structural fluctuations that occur on time scales out to several times the experimental window.⁷³

IV. Discussion

Could the change in the *Ht-M61A* dynamics be caused by the increase in viscosity of 5.1 M GuHCl compared to water? A detailed study of the viscosity dependence of CO vibrational dephasing for a number of heme proteins including *Ht-M61A* has been reported.⁸⁵ For many orders of magnitude increase in viscosity over aqueous protein solutions it was determined that the influence of viscosity on the observed spectral diffusion is very mild. For *Ht-M61A*, the dependence on viscosity goes as $\eta^{0.13}$, where η is the solution viscosity.⁸⁵ Furthermore, the homogeneous component is essentially unchanged by viscosity. In going from water to 5.1 M GuHCl, the viscosity only increases by 40%.⁸⁶ Given the very weak dependence of the vibrational dephasing on viscosity $\eta^{0.13}$ and the lack of influence of the viscosity on the homogeneous component, the change in viscosity is not responsible for the observed change in protein dynamics at 5.1 M GuHCl.

Insight into the influence of denaturation can be obtained by examining the results of placing *Ht-M61A* and other heme proteins in a glassy trehalose solvent.⁶² All of the heme proteins showed the same behavior. The homogeneous component of the FFCF (the extremely fast motions) remained essentially unchanged. However, the slower time scale dynamics within the experimental window, picoseconds to tens of picoseconds, were eliminated in the trehalose glass. Molecular dynamics simulations of the myoglobin-CO mutant H64V-CO (the distal histidine replaced with a valine) were conducted to understand the influence of a trehalose glassy solvent on protein dynamics and the vibrational echo observables.⁶² In the simulations, an aqueous protein solution was equilibrated and then the solvent was immobilized. The dynamics of the H64V-CO were investigated, and the FFCFs were determined for the immobilized solvent and a normal aqueous solution. The simulations reproduced the nature of the experimental results semiquantitatively. Like the experiments, the simulations showed that an ultrafast homogeneous component remained with the immobile solvent, but the slower time scale dynamics within the experimental and simulation windows were shut down. In addition, an analytical theory has been used to understand the viscosity dependence of protein dynamics using a breathing sphere model.^{87,88} The understanding that emerged from the simulations and theory showed that elimination of dynamics on the tens of picoseconds time scale is caused by locking up the surface topology of the protein. The internal motions of the protein structure depend on the ability of the surface topology to change.

The experiments in trehalose show how slowing or eliminating protein motions manifest themselves in the experimental observables. However, there are major differences between the trehalose experimental results and the results for denatured *Ht-M61A* shown in Figure 6. The key features of the trehalose experiments are that the homogeneous component is unchanged while the observable fluctuations on slower time scale are eliminated.⁶² In contrast, the denatured *Ht-M61A* data show a substantial change in the homogeneous component and the decay over the first few tens of picoseconds is not eliminated. The comparison between the linear spectra is significant. When *Ht-M61A* is put into glassy trehalose, the line width (fwhm) of the linear IR spectrum does not change and the peak position is only shifted by 3 cm^{-1} to higher frequency in trehalose compared to aqueous solution.⁶² This demonstrates that the basic

structure of the protein and the variations in structure about the average are almost unchanged when the surface topology is locked up. The ~ 10 ps time scale dynamics are pushed out to a long time beyond the experimental time window, but the structure is unchanged. This behavior is very different from the results for *Ht-M61A* in 5.1 M GuHCl. The *Ht-M61A* band shifts substantially to lower frequency and broadens considerably in going from the native to denatured protein. The shift in the position and change in width demonstrate that major structural changes have taken place in contrast to *Ht-M61A* in trehalose. Therefore, the changes in the FFCF observed for denatured *Ht-M61A* are caused by a change in structure, not by locking up the original native structure.

Looking at Table 1, the denatured protein's FFCF has a much smaller homogeneous line width (Γ), somewhat slower intermediate time scale dynamics (τ_1), and a much larger static component (Δ_s) compared to the native protein. One possible view of the denatured state is that it is comprised of a large number of structures that are each only slightly different from the native protein. Such a range of structures could account for the large increase in the line width of the denatured protein. However, this picture is inconsistent with the data. First, in addition to the increase in line width, the absorption spectrum of the fully denatured protein is shifted substantially to the red; thus, the average structure has changed. Furthermore, there is a large change in Γ , discussed in detail below, which demonstrates a substantial change from the native structure. The change in the intermediate time scale dynamics, ~ 10 ps, occurs at the onset of denaturation (see Table 1), indicating a change in structure. However, the large change in Γ , the change in the absorption peak position, and the increase in absorption line width are very different for the fully denatured protein than the mildly denatured and native proteins, demonstrating additional substantial changes in structure for the fully denatured protein.

Γ is reduced dramatically, by almost a factor of 2, in going from the native to the denatured protein. Γ is the motionally narrowed component of the FFCF. For a motionally narrowed contribution, the homogeneous line width is $\Gamma = \Delta^2\tau/\pi$, so it is not possible to determine from the experiments whether Δ or τ has changed or both. The 2D-IR vibrational echo experiments only determine the product, $\Delta^2\tau$.

Although it is not possible to determine Δ and τ from experiment, it is useful to examine a possible scenario using the results of molecular dynamics simulations. MD simulations have determined the FFCF for myoglobin-CO (MbCO).⁸⁹ In the MD simulations, Δ and τ for the motionally narrowed component were determined. From MD simulations of MbCO we know that the homogeneous component is caused by the very fast localized fluctuations of very small groups of atoms. These motions can be viewed as very low frequency vibrations, such as torsions of side chains. The MbCO MD simulation gave the motionally narrowed $\tau = 0.14$ ps. Note that $k_B T$ corresponds to 0.16 ps, where k_B is Boltzmann's constant and T is the absolute temperature. Thus, these very fast thermal fluctuations of small local modes have $\tau \approx h/k_B T$. It is reasonable to assume that τ is approximately the same for Mb and cyt *c*. Both Mb and cyt *c* are small globular heme proteins, and their very local motions might be expected to be similar.

Because the motionally narrowed component is due to very local motions of small groups of atoms, for heuristic purposes we will assume that τ does not change when the protein denatures. This is an assumption that will permit the discussion of a plausible explanation for the reduction in Γ when the protein unfolds. With the assumption that $\tau = 0.14$ ps, we can obtain

Δ for the native and denatured states. The values are 42 and 31 cm^{-1} , respectively. This decrease in Δ could be consistent with a hydrophobically collapsed state (see below) for the denatured protein in which the packing is more dense. The denser packing of the collapsed state could limit the amplitude of the local motions, thereby reducing Δ . Of course this argument is not rigorous, but it is indicative of a possible explanation for the large decrease in Γ with denaturation.

A hydrophobically collapsed denatured state is consistent with the funnel model of protein folding.^{7,8,11,12} As discussed in the Introduction, the opposite view of protein folding from the funnel model is folding or unfolding through a well-defined set of intermediates.^{2-5,10} In the sequential unfolding model, *cyt c* unfolds with as many as five intermediates through a sequence of unravelings of particular structural motifs.^{10,35} The denatured protein is unbundled with all regions exposed to solvent. Could this model be consistent with the IR experiments reported above? It is reasonable to assume that if the protein denatures in this manner, then there would be a wide variety of conformations that could result in the observed increase in the line width. The change in structure could result in an overall shift in the average frequency, although a red shift is generally associated with an increase electric field at the CO or increased back bonding from the iron-heme to the CO π^* antibonding molecular orbital.^{58,76,83,90,91} In MbCO, when the distal His moves away from the CO, the result is a blue shift.

The change in the 2D-IR results may not be consistent with a protein that is denatured through a sequence of unraveling intermediates. The denatured system should be more extended and floppy than the native protein. It is unlikely that such a system would have slower dynamics on the 10 ps time scale than the native protein. In a recent experiment, it was shown that cleaving a single disulfide bond in a heme protein led to a somewhat faster decay of the FFCF.⁵³ If large dissociative structural changes occur, then it would seem unlikely that the dynamics would slow. Furthermore, such a denatured state could have a wide range of configurations, but they might be expected to be sampled readily, which is inconsistent with the very large static component, Δ_s , of the FFCF found for the denatured state. Finally, consider the heuristic argument given above for the homogeneous component, Γ , and again assume that τ is unchanged. If this is the case, a less compact and less dense structure would yield a larger Δ and therefore a larger Γ , in contrast to the experimentally observed decrease in Γ for the denatured protein.

The arguments presented above, while qualitative, indicate that the state of the denatured protein is more consistent with a compact collapsed state suggested by funnel models than an unraveled expanded state suggested by the hierarchical unfolding models. The *Ht-M61A* results show that the denatured protein dynamics within the experimental window sample only a small portion of the total structural space. The implication is that motions over distances from a few Ångströms to less than or equal to ~ 20 Å⁸⁴ are slower compared to the native protein. However, the dynamics are not slowed to the extent that occurs when the protein's surface topology is completely locked up by a glassy solvent. The results shown in Figure 6 do not seem to be consistent with a picture in which the denatured protein has lost its native structure by unraveling, significantly expanding in size⁹² and becoming floppy, i.e., taking on a "random coil" form. The initial experiments presented in Figure 6 may indicate that the unfolded state of *Ht-M61A* is a compact, hydrophobicity driven collapsed state.

In the context of the funnel model, theoretical studies^{7,8} have suggested the existence of a collapsed and glassy unfolded state in close proximity of the native state, particularly with respect to the size of the protein. In the case of proteins in the *cyt c* family, theory⁶ and experiments⁹ indicate that the initial stage of folding is formation of a hydrophobicity induced collapsed state with most of the native contacts not formed. These contacts form subsequently along the folding pathway. For unfolding the predicted scenario is reversed. It has been suggested that for *cyt c* the hydrophobic heme pocket plays an important role in stabilization of the hydrophobic collapsed state.⁶

The theoretical study shows that because the heme-induced hydrophobic collapse occurs before a large fraction of native contacts are formed, the collapsed state can accommodate many non-native, possibly hydrophobic contacts.⁶ The hydrophobic collapsed state is predicted to be an important intermediate state. A similar conclusion was reached earlier by Takahashi and co-workers, who used small-angle X-ray scattering and resonance Raman to study folding of *cyt c*.^{9,66} It was found that along the folding pathway, the size of the protein decreases first without much change in the helical content. Subsequent to the collapse, the secondary structure is acquired.

The large static component of the FFCF for time scales longer than a few hundred picoseconds for *Ht-M61A* was observed for strongly denaturing conditions. Traditionally, denatured proteins were considered to exist in an extended conformation. A number of studies, however, have revealed residual structure in denatured proteins (for review, see ref 70). Gray, Winkler, and co-workers characterized distributions of dansyl fluorophore-heme distances in *Saccharomyces cerevisiae* iso-1-*cyt c*, a Class I *cyt c*, through a range of denaturing conditions and during folding. Their data reveal that denatured *cyt c* at equilibrium exists in a range of compact and extended conformations. In addition, both compact and extended conformations are observed in kinetic folding studies. These data indicate that even under strongly denaturing conditions a significant portion of the ensemble of *cyt c* structures exists in a collapsed state.^{32,69,70} It has been conjectured that the collapsed state can be glassy with slow collective dynamics.⁸ The large static component observed by the 2D-IR vibrational echoes when the denatured state is formed demonstrates that there is only a small amount of structural dynamics in the experimental time window (intermediate distance scale). The reduction in dynamics may be a signature of the hydrophobicity induced collapsed state.

V. Concluding Remarks

Here we examined the dynamics of denatured *cyt c* mutant *Ht-M61A* in comparison to the protein in its native form using ultrafast 2D-IR vibrational echo spectroscopy and linear IR absorption experiments. The similarity in trend between the CO peak shift curve and the CD curve in *cyt c* demonstrates that the vibrational stretching frequency of CO bound to *cyt c* is sensitive to the same types of changes in structure as a CD experiment.

The vibrational absorption lines are inhomogeneously broadened. The inhomogeneous broadening means that the ensemble of proteins has a heterogeneous distribution of structures. The 2D-IR vibrational echo experiment measures spectral diffusion, which occurs because of the interconversion of one protein structure to another. In terms of an energy landscape picture, under a particular set of equilibrium conditions, the protein occupies a broad rough minimum on the energy landscape. (There may be more than a single minimum that gives rise to structural substates^{93,94} as discussed for the native protein in

connection with Figure 5.) The roughness is caused by a collection of local minima between barriers of a range of heights. Some of the barriers are low enough that transitions are constantly taking place between the minima that correspond to variations in the protein structure within the experimental time window. Spectral diffusion is caused by transitions among the local minima. The time dependence of the spectral diffusion yields the time evolution of the protein structure.

In the time window of the 2D-IR vibrational echo experiments (~100 fs to ~100 ps), native *Ht-M61A* displays significant structural dynamics. Somewhat greater than 50% of the accessible structures that give rise to the inhomogeneous CO absorption line are sampled. When the protein is denatured in 5.1 M GuHCl, the inhomogeneous line is substantially broader than that for the native protein, which indicates a broader range of structures. The dynamics of the denatured protein in the experimental time window sample only a small fraction, less than 20%, of the increased range of structures. Therefore, a large fraction of the structural dynamics is occurring on time scales much greater than 100 ps.

In terms of the energy landscape picture, the results on the denatured protein in 5.1 M GuHCl indicate that the free energy landscape has become rather rugged or rough due to the appearance of deep minima, accompanied by barriers, in the region of the free energy landscape that contains the denatured state. Glassy behavior is a consequence of this ruggedness. Note that if ϵ is the variance that characterizes the ruggedness of the landscape, then configuration diffusion in the landscape varies as $\exp(-(\epsilon/k_B T)^2)$.⁹⁵ Thus, ruggedness can slow down configurational fluctuations drastically, giving rise to the much slower spectral diffusion in the denatured protein. The observed vibrational dynamics could be consistent with a hydrophobicity driven collapsed glassy state with such a rugged free energy landscape. Because glassy dynamics are predicted by landscape theory as being due to the appearance of ruggedness, it may be possible to estimate the ruggedness with inherent structure analysis⁹⁶ and explore the possible role of salt concentration in augmenting the ruggedness.

Clearly it will be important to fill in the 2D-IR vibrational echo data for concentrations of GuHCl between 3.2 and 5.1 M and concentrations > 5.1 M. The only limitations on obtaining additional data is that the experiments are complex and the mutant protein must be prepared in substantial quantity. While *Ht-M61A* under denaturing conditions may be in a hydrophobic collapsed state, there may be well defined non-native structures between those of the native state and the fully denatured state.⁹⁷ This is already suggested by the data shown in Figure 6 for the mildly denatured protein. These could be manifested as steps in the changes in dynamics as a function of GuHCl concentration. In addition, it will be important and interesting to perform the 2D-IR vibrational echo experiments on *Ht-M61A* using urea as a denaturant. Urea is believed to have a different mechanism for denaturation,^{13–17,98} and it is possible that the denatured state will be distinct and display different dynamics from the protein denatured with GuHCl.

The results presented in this paper are an important target for simulations. The time scales of the experiments, ~100 ps, are readily amenable to simulation. The relationship between simulations and the calculation of the 2D-IR vibrational echo spectra has been developed and applied to MbCO.^{58,62,83,99,100} Comparison of the simulation results for the native and denatured protein would provide a bench mark for simulations that are employed to understand protein folding and folding intermediates. If the simulations can reproduce the observed

behavior, then they should be able to provide a molecular level view of the structures responsible for the change in the dynamics observed for the denatured state.

Acknowledgment. We thank Professor Abani K. Bhuyan, School of Chemistry, University of Hyderabad, India, for providing the CD data shown in Figure 3A. This work was supported by the National Institutes of Health (2 R01 GM-061137-05), the Air Force Office of Scientific Research (F49620-01-1-0018), and the National Science Foundation (DMR 0652232). S.K. was supported by the Korea Research Foundation Grant funded by the Korean Government (MOE-HRD, basic Research Promotion Fund) (KRF-2006-C00038). K.L.B. acknowledges support from the National Institutes of Health (R01- GM63170).

References and Notes

- (1) Daggett, V.; Fersht, A. *Nat. Rev. Mol. Cell Biol.* **2003**, *4*, 497.
- (2) Daggett, V.; Fersht, A. R. *Trends Biochem. Sci.* **2003**, *28*, 18.
- (3) Laurents, D. V. a. B., R. L. *Biophys. J.* **1998**, *75*, 428.
- (4) Dill, K. A.; Shortle, D. *Annu. Rev. Biochem.* **1991**, *60*, 795.
- (5) Wallace, L. A.; Matthews, C. R. *BioPhys. Chem.* **2002**, *101*–102, 113.
- (6) Weinkam, P.; Zong, C. H.; Wolynes, P. G. *Proc. Natl. Acad. Sci. U.S.A.* **2005**, *102*, 12401.
- (7) Sasai, M.; Wolynes, P. G. *Phys. Rev. Lett.* **1990**, *65*, 2740.
- (8) Chahine, J.; Nymeyer, H.; Leite, V. B. P.; Socci, N. D.; Onuchic, J. N. *Phys. Rev. Lett.* **2002**, *88*, 168101.
- (9) Akiyama, S.; Takahashi, S.; Kimura, T.; Ishimori, K.; Morishima, I.; Nishikawa, Y.; Fujisawa, T. *Proc. Natl. Acad. Sci. U.S.A.* **2002**, *99*, 1329.
- (10) Hoang, L.; Bedard, S.; Krishna, M. M. G.; Lin, Y.; Englander, S. W. *Proc. Natl. Acad. Sci. U.S.A.* **2002**, *99*, 12173.
- (11) Onuchic, J. N.; LutheySchulten, Z.; Wolynes, P. G. *Annu. Rev. Phys. Chem.* **1997**, *48*, 545.
- (12) Bryngelson, J. D.; Onuchic, J. N.; Socci, N. D.; Wolynes, P. G. *Proteins-Struct. Funct. Genet.* **1995**, *21*, 167.
- (13) Elove, G. A.; Bhuyan, A. K.; Roder, H. *Biochemistry* **1994**, *33*, 6925.
- (14) Fedurco, M.; Augustynski, J.; Indiani, C.; Smulevich, G.; Antalick, M.; Bano, M.; Sedlak, E.; Glascock, M. C.; Dawson, J. H. *Biochim. Biophys. Acta, Proteomics Proteomics* **2004**, *1703*, 31.
- (15) Gupta, R.; Yadav, S.; Ahmad, F. *Biochemistry* **1996**, *35*, 11925.
- (16) Latypov, R. F.; Cheng, H.; Roder, N. A.; Zhang, J.; Roder, H. *J. Mol. Biol.* **2006**, *357*, 1009.
- (17) Russell, B. S.; Melenkivitz, R.; Bren, K. L. *Proc. Natl. Acad. Sci. U.S.A.* **2000**, *97*, 8312.
- (18) Smith, J. S.; Scholtz, J. M. *Biochemistry* **1996**, *35*, 7292.
- (19) Monera, O. D.; Cyril, M. K.; Hodges, R. S. *Protein Sci.* **1994**, *3*, 1984.
- (20) Massari, A. M.; McClain, B. L.; Finkelstein, I. J.; Lee, A. P.; Reynolds, H. L.; Bren, K. L.; Fayer, M. D. *J. Phys. Chem. B* **2006**, *110*, 18803.
- (21) Bren, K. L.; Kellogg, J. A.; Kaur, R.; Wen, X. *Inorg. Chem.* **2004**, *43*, 7934.
- (22) Jones, C. M.; Henry, E. R.; Hu, Y.; Chan, C. K.; Luck, S. D.; Bhuyan, A.; Roder, H.; Hofrichter, J.; Eaton, W. A. *Proc. Natl. Acad. Sci. U.S.A.* **1993**, *90*, 11860.
- (23) Sinibaldi, F.; Howes, B. D.; Piro, M. C.; Caroppi, P.; Mei, G.; Ascoli, F.; Smulevich, G.; Santucci, R. *J. Biol. Inorg. Chem.* **2006**, *11*, 52.
- (24) Kumar, R.; Prabhu, N. P.; Bhuyan, A. K. *Biochemistry* **2005**, *44*, 9359.
- (25) Droghetti, E.; Smulevich, G. *J. Biol. Inorg. Chem.* **2005**, *10*, 696.
- (26) Travaglini-Allocatelli, C.; Gianni, S.; Brunori, M. *Trends Biochem. Sci.* **2004**, *29*, 535.
- (27) Rischel, C.; Jorgensen, L. E.; Foldes-Papp, Z. *J. Phys. Condens. Matter* **2003**, *15*, 1725.
- (28) Hagen, S. J.; Latypov, R. F.; Dolgikh, D. A.; Roder, H. *Biochemistry* **2002**, *41*, 1372.
- (29) Bhuyan, A. K.; Udgaonkar, J. B. *J. Mol. Biol.* **2001**, *312*, 1135.
- (30) Panda, M.; Benavides-Garcia, M. G.; Pierce, M. M.; Nall, B. T. *Protein Sci.* **2000**, *9*, 536.
- (31) Jimenez, R.; Romesberg, F. E. *J. Phys. Chem. B* **2002**, *106*, 9172.
- (32) Lyubovitsky, J. G.; Gray, H. B.; Winkler, J. R. *J. Am. Chem. Soc.* **2002**, *124*, 5481.
- (33) Winkler, J. R. *Curr. Opin. Chem. Biol.* **2004**, *8*, 169.
- (34) Scott, R. A.; Mauk, A. G. *Cytochrome C: A Multidisciplinary Approach*; University Science Books: Sausalito, CA, 1996.

- (35) Krishna, M. M. G.; Lin, Y.; Rumbley, J. N.; Englander, S. W. *J. Mol. Biol.* **2003**, *331*, 29.
- (36) Pitsyn, O. B. *J. Mol. Biol.* **1998**, *278*, 655.
- (37) Varhac, R.; Antalík, M.; Bano, M. *J. Biol. Inorg. Chem.* **2004**, *9*, 12.
- (38) Russell, B. S.; Bren, K. L. *J. Biol. Inorg. Chem.* **2002**, *7*, 909.
- (39) Roccatano, D.; Daidone, I.; Ceruso, M. A.; Bossa, C.; Di Nola, A. *Biophys. J.* **2003**, *84*, 1876.
- (40) Droghetti, E.; Oellerich, S.; Hildebrandt, P.; Smulevich, G. *Biophys. J.* **2006**, *91*, 3022.
- (41) Dobson, C. M.; Sali, A.; Karplus, M. *Angew. Chem., Int. Ed.* **1998**, *37*, 868.
- (42) Anderson, J. L. R.; Chapman, S. K. *Dalton Trans.* **2005**, *13*, 9999.
- (43) Bren, K. L.; Gray, H. B. *J. Am. Chem. Soc.* **1993**, *115*, 10382.
- (44) Ambler, R. P. *Biochim. Biophys. Acta* **1991**, *1058*, 42.
- (45) Zheng, J.; Kwak, K.; Fayer, M. D. *Acc. Chem. Res.* **2007**, *40*, 75.
- (46) Finkelstein, I. J.; Zheng, J.; Ishikawa, H.; Kim, S.; Kwak, K.; Fayer, M. D. *Phys. Chem. Chem. Phys.* **2007**, *9*, 1533.
- (47) Park, S.; Kwak, K.; Fayer, M. D. *Laser Phys. Lett.* **2007**, *4*, 704.
- (48) Finkelstein, I. J.; Ishikawa, H.; Kim, S.; Massari, A. M.; Fayer, M. D. *Proc. Natl. Acad. Sci. U.S.A.* **2007**, *104*, 2637.
- (49) Massari, A. M.; Finkelstein, I. J.; Fayer, M. D. *J. Am. Chem. Soc.* **2006**, *128*, 3990.
- (50) Chung, H. S.; Khalil, M.; Smith, A. W.; Ganim, Z.; Tokmakoff, A. *Proc. Natl. Acad. Sci. U.S.A.* **2005**, *102*, 612.
- (51) Mukherjee, P.; Kass, I.; Arkin, I. T.; Zanni, M. T. *Proc. Natl. Acad. Sci. U.S.A.* **2006**, *103*, 3528.
- (52) Ishikawa, H.; Finkelstein, I. J.; Kim, S.; Kwak, K.; Chung, J. K.; Wakasugi, K.; Massari, A. M.; Fayer, M. D. *Proc. Natl. Acad. Sci. U.S.A.* **2007**, *104*, 16116.
- (53) Ishikawa, H.; Kim, S.; Kwak, K.; Wakasugi, K.; Fayer, M. D. *Proc. Natl. Acad. Sci. U.S.A.* **2007**, *104*, 19309.
- (54) Rella, C. W.; Rector, K. D.; Kwok, A. S.; Hill, J. R.; Schwettman, H. A.; Dlott, D. D.; Fayer, M. D. *J. Phys. Chem.* **1996**, *100*, 15620.
- (55) Fayer, M. D. *Annu. Rev. Phys. Chem.* **2001**, *52*, 315.
- (56) Wang, J.; Chen, J.; Hochstrasser, R. M. *J. Phys. Chem. B* **2006**, *110*, 7545.
- (57) Bredenbeck, J.; Helbing, J.; Kumita, J. R.; Woolley, G. A.; Hamm, P. *Proc. Natl. Acad. Sci. U.S.A.* **2005**, *102*, 2379.
- (58) Merchant, K. A.; Noid, W. G.; Akiyama, R.; Finkelstein, I.; Goun, A.; McClain, B. L.; Loring, R. F.; Fayer, M. D. *J. Am. Chem. Soc.* **2003**, *125*, 13804.
- (59) Karan, E. F.; Russell, B. S.; Bren, K. L. *J. Biol. Inorg. Chem.* **2002**, *7*, 260.
- (60) Fee, J. A.; Chen, Y.; Todaro, T. R.; Bren, K. L.; Patel, K. M.; Hill, M. G.; Gomez-Moran, E.; Loehr, T. M.; Ai, J.; Thöny-Meyer, L.; Williams, P. A.; Stura, E.; Sridhar, V.; McRee, D. E. *Protein Sci.* **2000**, *9*, 2074.
- (61) Wen, X.; Bren, K. L. *Biochemistry* **2005**, *44*, 5225.
- (62) Massari, A. M.; Finkelstein, I. J.; McClain, B. L.; Goj, A.; Wen, X.; Bren, K. L.; Loring, R. F.; Fayer, M. D. *J. Am. Chem. Soc.* **2005**, *127*, 14279.
- (63) Asbury, J. B.; Steinel, T.; Fayer, M. D. *J. Lumin.* **2004**, *107*, 271.
- (64) Pace, C. N.; Scholtz, J. M. Measuring the Conformational Stability of a Protein. In *Protein Structure: A Practical Approach*; Creighton, T. E., Ed.; Oxford University Press: New York, 1997; pp 299.
- (65) Karan, E. F.; Russell, B. S.; Bren, K. L. *J. Biol. Inorg. Chem.* **2002**, *7*, 260.
- (66) Takahashi, S.; Yeh, S. R.; Das, T. K.; Chi-Kin, C.; Gottfried, D. S.; Rousseau, D. L. *Nat. Struct. Biol.* **1997**, *4*, 44.
- (67) Elove, G. A.; Chaffote, A. F.; Roder, H.; Goldberg, M. E. *Biochemistry* **1992**, *31*, 6876.
- (68) Sosnick, T. R.; Mayne, L.; Hiller, R.; Englander, S. W. *Nat. Struct. Biol.* **1994**, *1*, 149.
- (69) Pletneva, E. V.; Gray, H. B.; Winkler, J. R. *J. Mol. Biol.* **2005**, *345*, 855.
- (70) Pletneva, E. V.; Gray, H. B.; Winkler, J. R. *Proc. Natl. Acad. Sci. U.S.A.* **2005**, *102*, 18397.
- (71) Rector, K. D.; Kwok, A. S.; Ferrante, C.; Tokmakoff, A.; Rella, C. W.; Fayer, M. D. *J. Chem. Phys.* **1997**, *106*, 10027.
- (72) Golonzka, O.; Khalil, M.; Demirdoven, N.; Tokmakoff, A. *Phys. Rev. Lett.* **2001**, *86*, 2154.
- (73) Bai, Y. S.; Fayer, M. D. *Phys. Rev. B* **1989**, *39*, 11066.
- (74) Dlott, D. D.; Fayer, M. D.; Hill, J. R.; Rella, C. W.; Suslick, K. S.; Ziegler, C. J. *J. Am. Chem. Soc.* **1996**, *118*, 7853.
- (75) Hill, J. R.; Dlott, D. D.; Rella, C. W.; Peterson, K. A.; Decatur, S. M.; Boxer, S. G.; Fayer, M. D. *J. Phys. Chem.* **1996**, *100*, 12100.
- (76) Hill, J. R.; Rosenblatt, M. M.; Ziegler, C. J.; Suslick, K. S.; Dlott, D. D.; Rella, C. W.; Fayer, M. D. *J. Phys. Chem.* **1996**, *100*, 18023.
- (77) Mukamel, S. *Principles of Nonlinear Optical Spectroscopy*; Oxford University Press: New York, 1995.
- (78) Mukamel, S. *Annu. Rev. Phys. Chem.* **2000**, *51*, 691.
- (79) Asbury, J. B.; Steinel, T.; Kwak, K.; Corcelli, S. A.; Lawrence, C. P.; Skinner, J. L.; Fayer, M. D. *J. Chem. Phys.* **2004**, *121*, 12431.
- (80) Kwak, K.; Park, S.; Finkelstein, I. J.; Fayer, M. D. *J. Chem. Phys.* **2007**, *127*, 124503.
- (81) Kwak, K.; Rosenthal, D. E.; Fayer, M. D. *J. Chem. Phys.* **2008**, accepted.
- (82) Woutersen, S.; Pfister, R.; Hamm, P.; Mu, Y.; Kosov, D. S.; Stock, G. *J. Chem. Phys.* **2002**, *117*, 6833.
- (83) Merchant, K. A.; Noid, W. G.; Thompson, D. E.; Akiyama, R.; Loring, R. F.; Fayer, M. D. *J. Phys. Chem. B* **2003**, *107*, 4.
- (84) Bu, Z.; Neumann, D. A.; Lee, S. H.; Brown, C. M.; Engelman, D. M.; Han, C. C. *J. Mol. Biol.* **2000**, *301*, 525.
- (85) Finkelstein, I. J.; Massari, A. M.; Fayer, M. D. *Biophys. J.* **2007**, *92*, 3652.
- (86) Kawahara, K.; Tanford, C. *J. Biol. Chem.* **1966**, *241*, 3228.
- (87) Rector, K. D.; Jiang, J.; Berg, M.; Fayer, M. D. *J. Phys. Chem. B* **2001**, *105*, 1081.
- (88) Rector, K. D.; Engholm, J. R.; Rella, C. W.; Hill, J. R.; Dlott, D. D.; Fayer, M. D. *J. Phys. Chem. A* **1999**, *103*, 2381.
- (89) Merchant, K. A.; Thompson, D. E.; Xu, Q.-H.; Williams, R. B.; Loring, R. F.; Fayer, M. D. *Biophys. J.* **2002**, *82*, 3277.
- (90) Augspurger, J. D.; Dykstra, C. E.; Oldfield, E. *J. Am. Chem. Soc.* **1991**, *113*, 2447.
- (91) Hill, J. R.; Dlott, D. D.; Fayer, M. D.; Rella, C. W.; Rosenblatt, M. M.; Suslick, K. S.; Ziegler, C. J. *J. Phys. Chem.* **1996**, *100*, 218.
- (92) Tsong, T. Y. *J. Biol. Chem.* **1974**, *249*, 1988.
- (93) Frauenfelder, H.; Parak, F.; Young, R. D. *Annu. Rev. Biophys. Chem.* **1988**, *17*, 471.
- (94) Frauenfelder, H.; Sligar, S. G.; Wolynes, P. G. *Science* **1991**, *254*, 1598.
- (95) Zwanzig, R. *Proc. Natl. Acad. Sci. U.S.A.* **1988**, *85*, 2029.
- (96) DeBenedetti, P. G.; Stillinger, F. H. *Nature* **2001**, *410*, 259.
- (97) Russell, B. S.; Melenkivitz, R.; Bren, K. L. *Proc. Natl. Acad. Sci. U.S.A.* **2000**, *97*, 8312.
- (98) Gianni, S.; Brunori, M.; Travaglini-Allocatelli, C. *Protein Sci.* **2001**, *10*, 1685.
- (99) Williams, R. B.; Loring, R. F.; Fayer, M. D. *J. Phys. Chem. B* **2001**, *105*, 4068.
- (100) Finkelstein, I. J.; Goj, A.; McClain, B. L.; Massari, A. M.; Merchant, K. A.; Loring, R. F.; Fayer, M. D. *J. Phys. Chem. B* **2005**, *109*, 16959.